JVSTB Journal of Vacuum Science & Technology B

Effect of surface pretreatment of submicron contact hole on selective tungsten chemical vapor deposition

WenKuan Yeh, MaoChieh Chen, and MouShiung Lin

Citation: Journal of Vacuum Science & Technology B **14**, 167 (1996); doi: 10.1116/1.589021
View online: http://dx.doi.org/10.1116/1.589021
View Table of Contents: http://scitation.aip.org/content/avs/journal/jvstb/14/1?ver=pdfcov
Published by the AVS: Science & Technology of Materials, Interfaces, and Processing

Articles you may be interested in

Effects of hydrogen surface pretreatment of silicon dioxide on the nucleation and surface roughness of polycrystalline silicon films prepared by rapid thermal chemical vapor deposition
Appl. Phys. Lett. **69**, 485 (1996); 10.1063/1.118148

Selectivity loss during tungsten chemical vapor deposition: The role of tungsten pentafluoride
J. Vac. Sci. Technol. A **7**, 621 (1989); 10.1116/1.575854

New insights on nucleation of tungsten on insulators during selective chemical vapor deposition
Appl. Phys. Lett. **50**, 965 (1987); 10.1063/1.98000

Diffusion barrier properties of thin selective chemical vapor deposited tungsten films
J. Vac. Sci. Technol. B **4**, 1369 (1986); 10.1116/1.583460

Barrier effect of selective chemical vapor deposited tungsten films
J. Vac. Sci. Technol. B **4**, 1175 (1986); 10.1116/1.583478

Re-register for Table of Content Alerts

Create a profile.

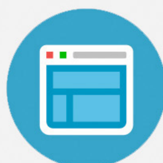

Sign up today!

Redistribution subject to AVS license or copyright; see http://scitation.aip.org/termsconditions. Download to IP: 140.113.38.11 On: Thu, 01 May 2014 10:39:31

Effect of surface pretreatment of submicron contact hole on selective tungsten chemical vapor deposition

Wen-Kuan Yeh and Mao-Chieh Chen
Department of Electronics Engineering, National Chiao Tung University and National Nano Device Laboratory, 1001 University Road, Hsinchu, Taiwan, Republic of China

Mou-Shiung Lin
Taiwan Semiconductor Manufacturing Company, Hsinchu, Taiwan, Republic of China

(Received 14 November 1994; accepted 11 November 1995)

The effects of various predeposition treatments of silicon substrates on selective tungsten chemical vapor deposition were investigated using the silane reduction process. The predeposition treatments include HF or buffered HF wet etch and/or NF_3 plasma etch. The experimental results show remarkable differences in the initial nucleation of W and the smoothness of the W surface and the W/Si interface among the various treatments, as revealed by scanning electron microscope inspection and atomic force microscope analysis. Plasma etch leads to a rough W/Si interface while wet treatment with HF dip results in a fairly smooth interface. The experimental results show that better $I-V$ characteristics for the W/n-Si Schottky contact can be obtained by the wet etch treatment prior to the W deposition. The reverse bias junction leakage for the wet etch pretreated W/p^+n junction diode is smaller than that of the plasma pretreated diode. In addition, the substrate surface treatments were found to result in Si consumption of various degrees. © *1996 American Vacuum Society.*

I. INTRODUCTION

Selective tungsten chemical vapor deposition (W-CVD) is one of the most attractive techniques for filling deep submicron contact holes and via holes for ultralarge scale integrated (ULSI) applications. Selective W-CVD can be performed using the hydrogen (H_2) reduction[1] or silane (SiH_4) reduction[2,3] of tungsten hexafluoride (WF_6).

Selective W-CVD, using the H_2 reduction process, can result in a high reactivity of WF_6 toward the silicon substrate. Thus, it causes excessive Si consumption, encroachment at the Si/SiO_2 interface, and worm hole formation in the contact regions.[4,5] These disadvantages do not occur during the silane reduction process.[6] For both processes, the silicon displacement reaction takes place at the initial stage. Then, after a certain thickness of tungsten is formed, the silicon displacement reaction is self-limited by the tungsten film.[7] It is expected and experimentally confirmed that the surface preparation has a profound effect on the Si consumption during W-CVD.

The common predeposition treatments of a Si substrate include HF etch, buffered HF(BHF) etch, and plasma etch. The Si(100) surface is isotropically and microscopically rough after being treated in dilute HF;[8,9] it becomes even rougher when it is treated in BHF solution, due to (111) facet formation.[10,11] The Si(100) surface after HF dip is mostly hydrogen passivated,[12] while the fluorine coverage on the surface is only about 10% and can be further reduced to a few percent by deionized (DI) water rinse in 10 min.[13] However, this minority fluorine plays a significant role in enhancing silicon surface oxidation.[14] During the DI water rinse, the Si–F species on the HF treated Si(100) surface rapidly interact with H_2O to form Si–OH groups, and the condensation of Si–OH forms Si–O–Si bridges and SiO_2.[15,16] The BHF treated Si(100) surface was found to be almost purely hydrogen terminated[17] and extremely stable against reoxidation and contamination in air.[18] After plasma etch in dilute NF_3 gas, the Si surface was damaged and covered with fluorine species.[19,20]

The purpose of this article is to clarify the effects of various substrate surface treatments prior to conducting selective W-CVD using the silane reduction process on a contact hole patterned substrate. The predeposition treatments include wet etch with dilute HF or BHF and/or NF_3 plasma etch. The experimental results show remarkable differences in the initial nucleation stage of W as well as the smoothness of the W/Si interface among the various predeposition treatments.

II. EXPERIMENTAL DETAILS

The starting material was p-type ⟨100⟩ oriented Si wafers with 8–12 Ω cm nominal resistivity. After RCA standard cleaning, the wafers were oxidized thermally to grow a 1500 Å thickness of SiO_2, followed by deposition of 4500 Å of Borophosphosilicate glass (BPSG). A p^+ junction implant was carried out by BF_2^+ implantation at 30 keV to a dose of 3×10^{15} cm^{-2} followed by furnace annealing at 900 °C for 30 min in an N_2 ambient. Contact holes with sizes ranging from 0.6 to 1.2 μm were then defined on the wafers using the conventional photolithographic technique. Prior to selective W-CVD, the wafers were dipped in diluted HF (2%) or BHF solution, with a pH value of 4.5 (7:1 mixture of 50 wt % HF in H_2O and 40 wt % NH_4F in H_2O for 10–30 s, followed by a rinse in deionized water for 2 min. The wafers were then loaded into the load-locked cold wall W-CVD system within 5 min.

In this work, the predeposition plasma etch was conducted with the following conditions: rf power: 30–50 W; total gas pressure: 100 mTorr; NF_3 flow rate: 12 sccm; and

 0734-211X/96/14(1)/167/7/$10.00 ©1996 American Vacuum Society

Redistribution subject to AVS license or copyright; see http://scitation.aip.org/termsconditions. Download to IP: 140.113.38.11 On: Thu, 01 May 2014 10:39:31

N_2 flow rate: 72 sccm. After the plasma etch, the wafers were transferred by a robot arm from the plasma etch chamber to the deposition chamber without expose to the atmosphere. The base pressure of the CVD chamber is 10^{-6} Torr. Typical conditions for the W-CVD conducted in this work are as follows: substrate temperature: 280–320 °C; total gas pressure: 100 mTorr; WF_6 flow rate: 20–30 sccm; SiH_4 flow rate: 10–20 sccm; and H_2 carrier gas flow rate 1000 sccm. After the selective W-CVD, Al metalization was applied, followed by a 30 min sintering at 400 °C. The nucleation of W and the thickness of the tungsten film were determined by use of a scanning electron microscope (SEM). The surface roughness of the W film was inspected by using an atomic force microscope (AFM). The Fourier transform infrared (FTIR) differential spectrum was used to detect the formation of various bonds on the Si surface.

III. RESULTS

A. Surface microroughness after predeposition treatment

Figure 1 depicts the Si substrate surface after various pre-

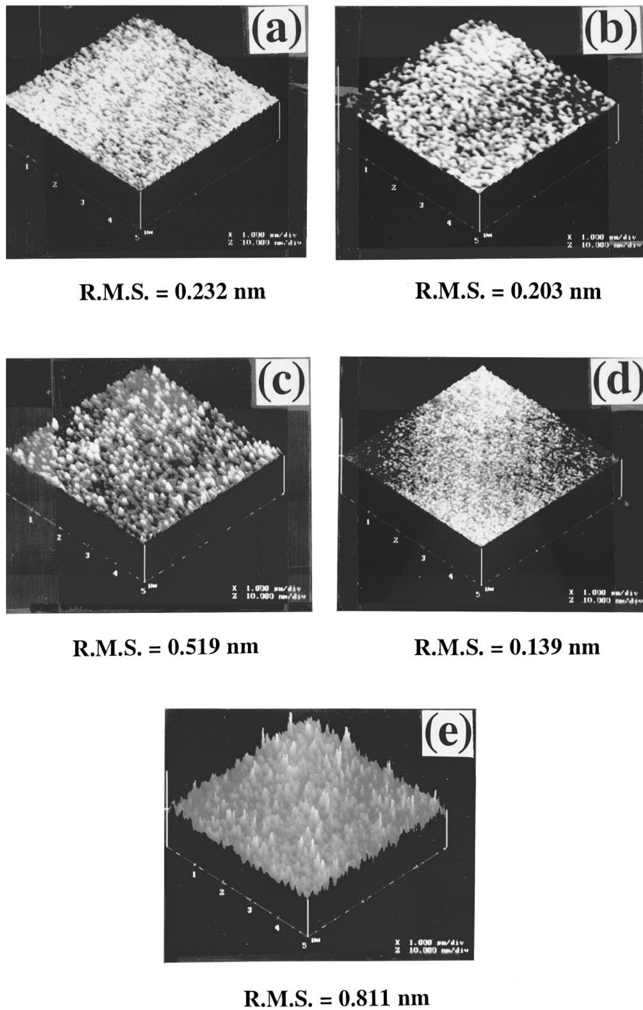

FIG. 1. Silicon surface microroughness with and without predeposition treatments as determined by an AFM: (a) without pretreatment, (b) with HF dip, (c) with BHF dip, (d) with HF dip followed by 30 W NF_3 plasma etch, and (e) same as (d) but with 50 W plasma etch.

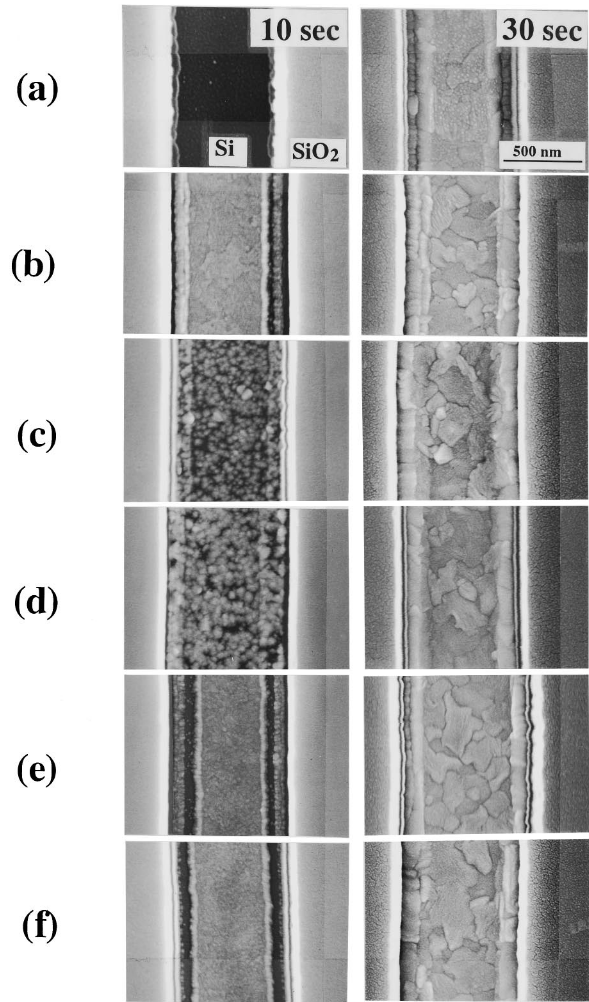

FIG. 2. The initial nucleation stage of 10 (left) and 30 s (right) selective W-CVD on Si surfaces inside submicron trench which had been treated with (a) HF dip followed by DI water rinse, (b) BHF dip followed by DI water rinse, (c) HF dip followed by DI water rinse and subsequent NF_3 plasma etch, (d) BHF dip followed by DI water rinse and subsequent NF_3 plasma etch, (e) HF dip only, and (f) BHF dip only.

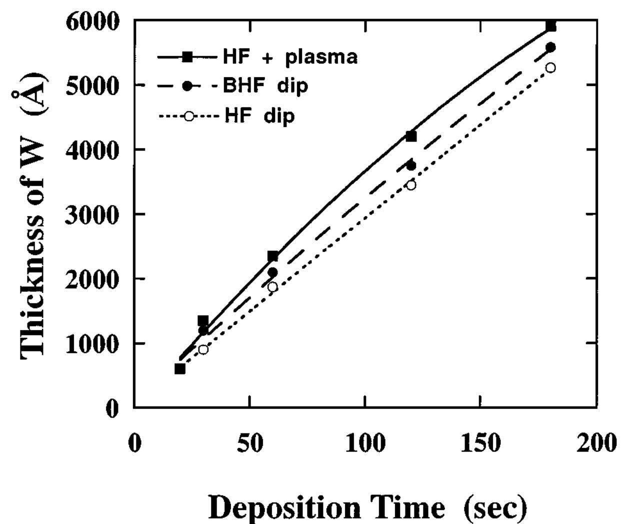

FIG. 3. Thickness of tungsten film vs deposition time of W-CVD for various predeposition surface treatments.

Redistribution subject to AVS license or copyright; see http://scitation.aip.org/termsconditions. Download to IP: 140.113.38.11 On: Thu, 01 May 2014 10:39:31

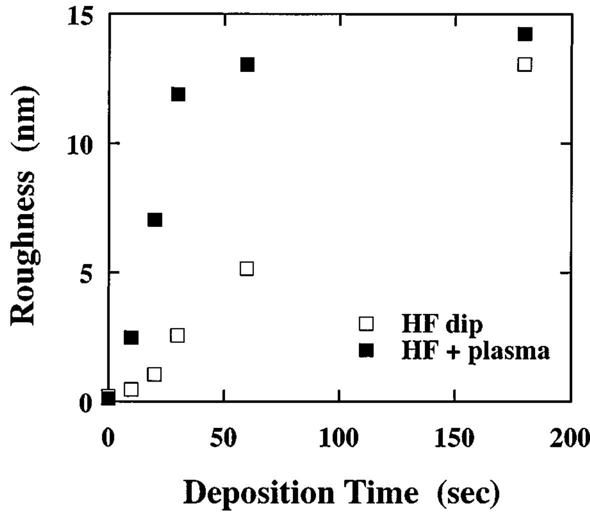

FIG. 4. Surface roughness of tungsten film vs deposition time of W-CVD for HF dipped substrates with and without additional NF_3 plasma etch.

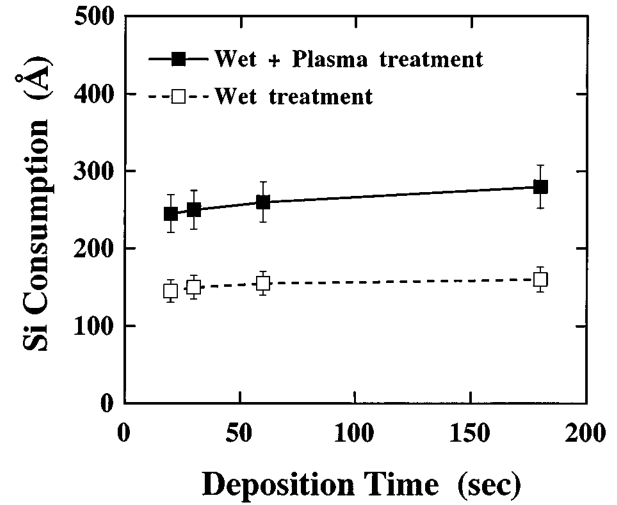

FIG. 6. Si consumption vs deposition time of W-CVD for two different predeposition treatments.

deposition treatments, as determined by an AFM. It can be seen that the HF dipped surface [root-mean-square roughness rms=0.203 nm, as shown in Fig. 1(b)] is much smoother than the BHF dipped surface [rms=0.519 nm, as shown in Fig. 1(c)]. It should be noted that, in contrast with the HF-cleaned Si surface, whereon only the surface oxide was selectively removed, BHF attacks bulk silicon anisotropically.[8] The use of buffered HF may be ill-advised in attempting to prepare atomically flat (100) surfaces, since (111) facets develop upon the BHF etch. Increased surface roughness has been directly observed after BHF etch. A very smooth Si surface was obtained [rms=0.139 nm, as shown in Fig. 1(d)] after the 30 W plasma etch following the HF dip; however, the surface became very rough [rms=0.811 nm, as shown in Fig. 1(e)] when the plasma power was raised from 30 to 50 W.

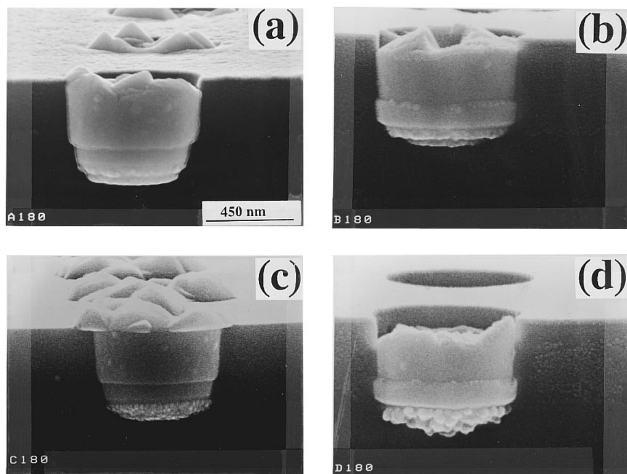

FIG. 5. Cross section SEM micrographs showing W deposition in submicron contact hole for various substrate pretreatments: (a) HF dip, (b) BHF dip, (c) HF dip+plasma etch, and (d) BHF dip+plasma etch. The deposition time was 180 s.

B. Initial nucleation stage of W-CVD

The SEM micrographs illustrated in Fig. 2 show the initial nucleation stage of 10 (left) and 30 s (right) selective W-CVD on the Si surface inside submicron trench which had received various predeposition treatments. The wet etch with dilute HF dip followed by DI water rinse resulted in a longer incubation time (or delayed nucleation of W) [Fig. 2(a)]. The incubation time was shortened when BHF was used instead

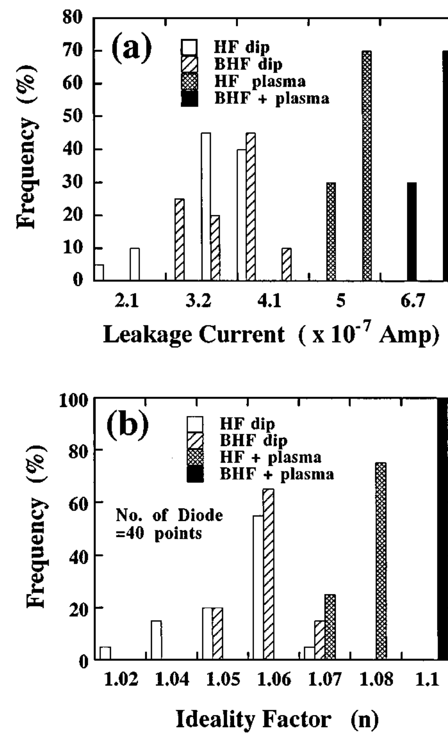

FIG. 7. The histograms showing the distribution of (a) reverse biased current measured at −5 V, and (b) forward ideality factor, for the W/n-Si Schottky diodes. The Si substrates were pretreated with four different wet and/or plasma etches.

Redistribution subject to AVS license or copyright; see http://scitation.aip.org/termsconditions. Download to IP: 140.113.38.11 On: Thu, 01 May 2014 10:39:31

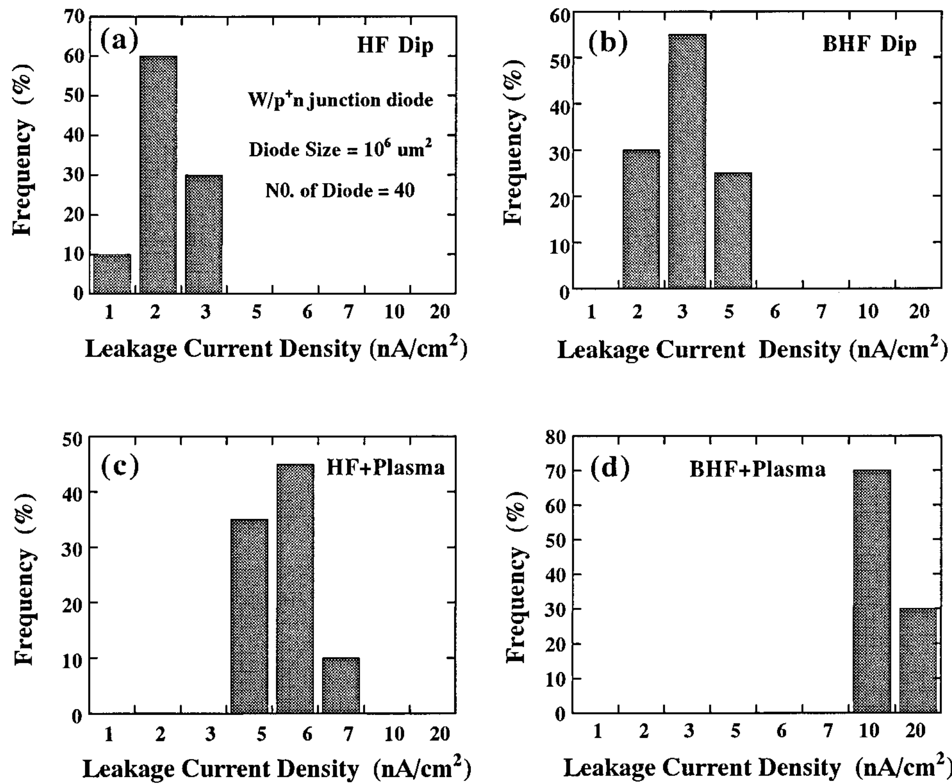

FIG. 8. The histograms showing the distribution of reverse leakage current density measured at −5 V for the W/p^+n junction diodes. The Si substrates were pretreated with four different wet and/or plasma etches.

of HF [Fig. 2(b)]. The NF_3 plasma treatment further shortened the incubation time [Figs. 2(c) and 2(d)]; the W nucleation sites can be clearly observed after 10 s W-CVD, and its morphology also looks different from those of the HF and BHF etched samples. The substrates with wet treatments, either HF or BHF, but without DI water rinse also resulted in very short incubation times [Figs. 2(e) and 2(f)]; it can be seen that the nucleation has rapidly developed into a smooth W film after 10 s of W-CVD. Figure 3 shows the thickness of tungsten film versus deposition time of W-CVD for various predeposition surface treatments. The incubation time is different during the nucleation stage of W for the various pretreatment cases, but the deposition rates of W-CVD eventually became nearly equal (about 1800 Å/min). Because of the different initial nucleation stages of W-CVD, the surface roughness of the W film is also different in the early period of CVD (e.g., in the first 60 s). However, surface morphologies for all samples did not show obvious differences after a prolonged deposition. Figure 4 shows the surface roughness of the W film versus deposition time of W-CVD for HF dipped substrates with and without additional NF_3 plasma etch, as obtained by AFM.

C. Tungsten/silicon interface

Figure 5 shows the cross section SEM micrographs for the W-filled contact holes with 0.6 μm size. The HF and BHF etches resulted in a belt ring around the sidewall of the contact hole, due to the different etching rates between the undoped SiO_2 and BPSG films. It can also be seen that wet etch with HF dip resulted in a very smooth W/Si interface [Fig. 5(a)], while the plasma etch led to a rough W/Si interface [Figs. 5(c) and 5(d)]. The BHF etch resulted in slightly more consumption of Si compared to the HF etch, because NH_4F will attack the bulk Si anisotropically [Fig. 5(b)]. The subsequent plasma etch will cause further Si consumption depending on the plasma power; higher power resulted in increased Si consumption. The Si consumption was independent of the deposition time of W-CVD, as revealed in Fig. 6. The Si displacement process takes place only at the beginning of W-CVD, and the thickness of Si consumption remained constant during the entire deposition time of W-CVD at temperatures below 400 °C.[21]

D. $I-V$ characteristics

The current–voltage characteristics were measured on the W/n-Si Schottky contact diodes and W/p^+n junction diodes, which were fabricated by selective W-CVD on the variously pretreated Si substrates with defined diode areas of 1000 $\times 1000$ μm^2. At least 40 randomly chosen diodes were measured in each case. Figure 7 illustrates the histograms showing the distribution of the reverse biased current and forward ideality factor for the W/n-Si Schottky contact diodes. The Schottky diodes with wet treatment prior to the W deposition revealed better $I-V$ characteristics than those with additional plasma treatment. This result is consistent with the SEM observation, as shown in Fig. 5, that the predeposition plasma

Redistribution subject to AVS license or copyright; see http://scitation.aip.org/termsconditions. Download to IP: 140.113.38.11 On: Thu, 01 May 2014 10:39:31

treatment resulted in a fairly rough W/Si interface after the W deposition. It also shows that the Schottky diodes, made with wet treatment, have a scattered distribution of reverse current and ideality factor.

Figure 8 illustrates the histograms showing the distribution of the reverse leakage current density measured at -5 V for the W/p^+n junction diodes with various predeposition substrate treatments. The average reverse leakage current density for the junction diodes with HF treatment is 2 nA/cm^2. The reverse leakages for the junction diodes with wet treatment and an additional plasma treatment were found to be about three times larger than those of the diodes which did not receive the plasma etch. The plasma treatment tended to result in more Si consumption and a rough W/Si interface after the selective W-CVD. This is presumably the main reason for the increased reverse leakage for the shallow junction diodes.

IV. DISCUSSION

In general, only two chemistries have been seriously studied with respect to selective tungsten deposition: H_2/WF_6 (hydrogen reduction process) and SiH_4/WF_6 (silane reduction process). In this work, the SiH_4 reduction process was used in order to avoid the HF by-product of the H_2 reduction process which would cause undesirable excessive Si consumption. Nonetheless, in both processes, the first reaction that occurs between Si and WF_6 is the so-called Si displacement reaction.

During the Si displacement reaction, WF_6 first dissociates on the Si surface forming $WF_x(x<6)$ adsorbed on the surface, and then further reduces to W. At the same time, Si is converted into $SiF_x(x\geq 1)$ and further changes to SiF_4. The overall process can be expressed as[7]

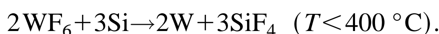

$$2WF_6+3Si\rightarrow 2W+3SiF_4 \quad (T<400\,^\circ C).$$

The Si surface must be fluorided or hydrided first so as to adsorb the WF_6 molecule. The HF-cleaned Si surface is mostly hydrogen passivated. The hydrogen terminated surface is surprisingly stable in the air towards reoxidation. The FTIR spectrum shown in Fig. 9(a) confirms the existance of the Si–H bond (2080–2160 cm^{-1}). In fact, small amounts of fluorine also existed on the HF treated Si surface, and the fluorine-terminated surface was oxidized rapidly in water.[22] The fluorine-terminated surfaces are much more reactive with water than the hydrogen-terminated surfaces. When the HF dipped wafer is rinsed by deionized water, the flourine-terminated surface (Si–F bond) will be converted to Si–OH species. The FTIR spectrum shown in Fig. 9(b) shows that the HF-cleaned Si surface produced Si–OH bond (3200–3700 cm^{-1}) after DI water rinse for 2 min, which is consistent with those reported in the literature.[23] Condensation of Si–OH forms Si–O–Si bridges which is the prestage of SiO_x.[15,16] The native oxide (SiO_x) will interfere with the incubation of tungsten and increase the nucleation time of W-CVD [Fig. 2(a)].

In contrast to the HF-cleaned Si substrate, the Si surface after BHF dip was found to be almost purely hydrogen terminated which is extremely stable against reoxidation and contamination in the air. The existance of the Si–H bond is confirmed, as shown in Fig. 10(a). The BHF-cleaned surface, which does not exhibit surface fluorine, ought to be stable during the subsequent water rinse.[14] Figure 10(b) shows that the BHF-cleaned and DI water rinsed surface did not reveal any obvious Si–OH peak. Therefore, the incubation time of W-CVD on the BHF-cleaned Si surface followed by DI water rinse [Fig. 2(b)] is shorter than that on the HF-cleaned and DI water rinsed Si surface [Fig. 2(a)]. If the wet etching of HF or BHF is not followed by the DI water rinse, the Si–H and Si–F bonds produced on the HF-cleaned Si surface and the Si–H bonds produced on the BHF-cleaned Si surface would attract the WF_6 molecules to the Si surface and enhance the nucleation of W film [Figs. 2(e) and 2(f)].

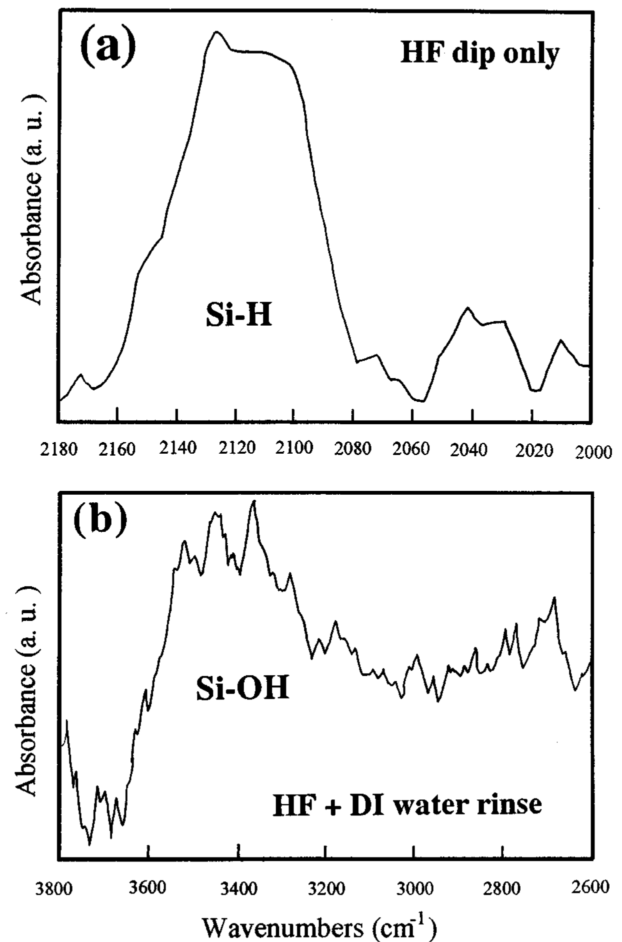

FIG. 9. FTIR differential spectrum for the Si surface after (a) HF dip only and (b) HF dip followed by deionized water rinse for 2 min.

For the plasma etched substrate, the NF_3 plasma breaks the Si–Si bonds on the Si surface and produces a large amount of surface damage.[19,24] This surface damage, which has lower potential energy, will easily attract the WF_6 species to react with Si and further proceed with the nucleation of W islands. The W islands will cause nonuniform Si consumption leading to rough W/Si interface. Although both the Si–H and Si–F dangling bonds exist on the HF-cleaned Si substrate, the WF_6 molecules are first attracted to the Si–F bond

Redistribution subject to AVS license or copyright; see http://scitation.aip.org/termsconditions. Download to IP: 140.113.38.11 On: Thu, 01 May 2014 10:39:31

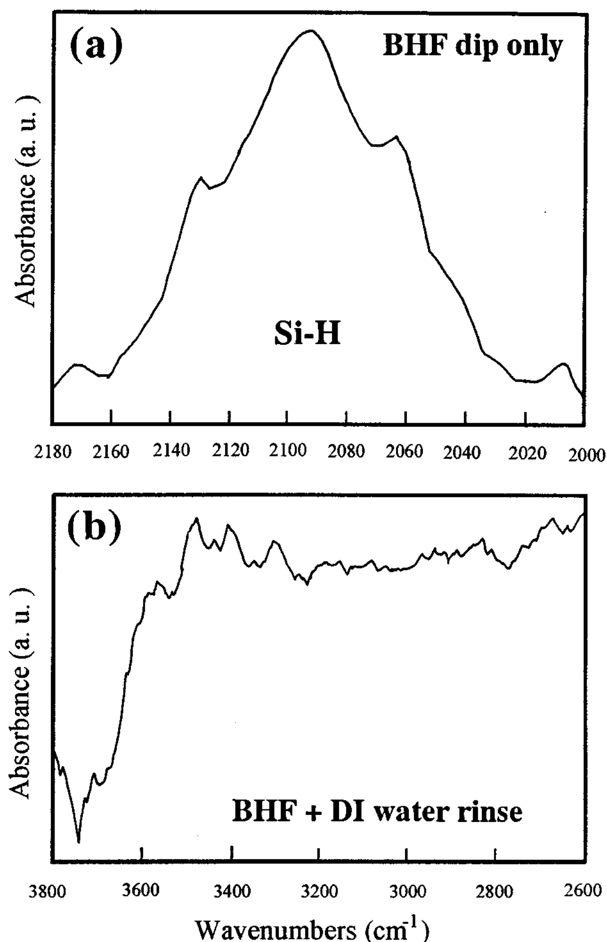

FIG. 10. FTIR differential spectrum for the Si surface after (a) BHF dip only and (b) BHF dip followed by deionized water rinse for 2 min.

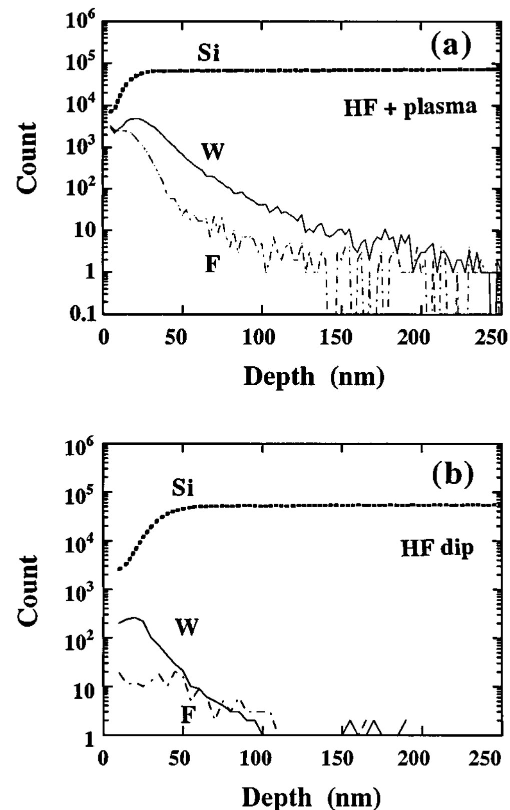

FIG. 11. SIMS depth profiles of the CVD W films deposited on Si substrates which was (a) HF dipped followed by DI water rinse and then NF_3 plasma etched, and (b) HF dipped followed by DI water rinse. The deposition time of the W-CVD was 20 s.

which has a lower potential energy[25] and proceed with the displacement reaction. Silicon reduces the WF_6 molecules, leading to the deposition of a W film. The tungsten surface, either by retaining some of the fluorine or adsorbing more WF_6 species, is highly fluorinated; thus, SiH_4 reacts with this surface to form W, leaving SiF_4 and H_2 on the surface.[26] On the other hand, the WF_6 molecules need more energy to break the Si–H bond that exists on the Si surface. When the Si–H bond is broken, the WF_6 species will react with the H atom and reproduce the HF species which will cause Si consumption to some extent, like the H_2 reduction process. In all, during the initial nucleation stage of W film, the Si displacement process which proceeds on the Si–F bond, and the H_2 reduction process which proceeds on the Si–H bond, will occur simultaneously until the Si surface is entirely covered with a W film. After that, the W film deposition is completely taken over by the silane reduction process. Figure 11 shows the secondary ion mass spectroscopy (SIMS) depth profiles of the CVD W films deposited on the HF dipped and DI water rinsed Si substrate with and without a subsequent NF_3 plasma etch. The deposition time of the W-CVD was 20 s. A very high concentration of fluorine is observed in the W film deposited on the plasma etched substrate [Fig. 11(a)]. On the other hand, a relatively thin W film was deposited on the HF-cleaned and DI water rinsed Si substrate, and the film contained a very low concentration of fluorine [Fig. 11(b)].

V. SUMMARY

The Si substrate surface condition imposes great influence on the behavior of W-CVD. The experimental results indicate remarkable differences in the initial nucleation stage of W as well as the smoothness of W/Si interface among the various predeposition treatments of substrate surfaces. Both Si–H and Si–F bonds were produced on the HF-cleaned Si substrate surfaces, while only Si–H bonds were produced on the BHF-cleaned surfaces; either the Si–H or the Si–F bonding enhanced the W nucleation. If the HF-dipped wafer is followed by DI water rinse, the surface will produce a large number of Si–OH species which will retard the nucleation of W. On the other hand, if the BHF-dipped wafer is followed by DI water rinse, the surface remained to be hydrogen terminated and the nucleation of W still can be enhanced. With additional NF_3 plasma etching following the wet treatment, the large amount of surface damage produced on the Si substrate will attract the WF_6 molecules to react with Si and eventually lead to the nucleation of W islands. Thus, it was found that the wet etch of the Si substrate using dilute HF resulted in an increased incubation time and a very smooth W/Si interface. The plasma etch resulted in a shortened in-

Redistribution subject to AVS license or copyright; see http://scitation.aip.org/termsconditions. Download to IP: 140.113.38.11 On: Thu, 01 May 2014 10:39:31

cubation time and a rough interface. In addition, better $I-V$ characteristics were found for the W/n-Si Schottky diodes and the W/p^+n junction diodes with the Si substrates wet etched in dilute HF prior to the selective W-CVD rather than etched in NF_3 plasma.

ACKNOWLEDGMENT

This work was supported by the National Science Council (ROC) under Contract No. NSC84-2622-E009-007-1.

[1]C. M. McConica and K. Krishnamani, J. Electrochem. Soc. **132**, 2542 (1986).
[2]R. F. Foster, S. Tseng, L. Lane, and K. Y. Ahn, *Tungsten Workshop III* (Materials Research Society, Pittsburgh, 1988), p. 69.
[3]Y. Kusumoto, K. Takakuwa, H. Hashinokuchi, T. Ikuta, and I. Nakayama, *Tungsten Workshop III* (Materials Research Society, Pittsburgh, 1987), p. 103.
[4]W. T. Stacy, E. K. Broadbent, and M. H. Norcott, J. Electrochem. Soc. **132**, 444 (1985).
[5]R. A. Levy, M. L. Green, P. K. Gallagher, and Y. S. Ali, J. Electrochem. Soc. **133**, 1905 (1986).
[6]R. S. Rosler, J. Mendonca, and M. J. Rice, Jr., J. Vac. Sci. Technol. B **6**, 1721 (1988).
[7]E. K. Broadbent and C. L. Ramiller, J. Electrochem. Soc. **131**, 1427 (1984).
[8]G. J. Pietsch, U. Kohler, and M. Henzler, J. Appl. Phys. **73**, 4797 (1993).
[9]Y. J. Chabal, G. S. Higashi, and K. Raghavachari, J. Vac. Sci. Technol. A **7**, 2104 (1989).
[10]D. Graf, M. Brohl, S. Bauer-Mayer, A. Ehlert, P. Wagner, and A. Schnegg, Mater. Res. Soc. Symp. Proc. **315**, 23 (1993).
[11]Y. J. Chabal, Mater. Res. Soc. Symp. Proc. **259**, 349 (1992).
[12]M. Grundner and H. Jacob, Appl. Phys. A **39**, 73 (1986).
[13]T. Sunada, T. Yasaka, M. Takakura, T. Sugiyama, and M. Hirose, Jpn. J. Appl. Phys. **29**, L2408 (1990).
[14]R. A. Haring and M. Liehr, J. Vac. Sci. Technol. A **10**, 802 (1992).
[15]D. Graf, M. Grunder, and R. Schulz, J. Vac. Sci. Technol. A **7**, 808 (1989).
[16]D. Graf, M. Grunder, and R. Schulz, J. Appl. Phys. **68**, 5155 (1990).
[17]P. Dumas and Y. J. Chabal, J. Vac. Sci. Technol. A **10**, 2160 (1992).
[18]M. Morita, T. Ohmi, E. Hasegawa, M. Kawakami, and M. Ohwada, J. Appl. Phys. **68**, 1272 (1990).
[19]W. Kern, *Handbook of Semiconductor Wafer Cleaning Technology* (Noyes, Park Road, NJ, 1993), pp. 224–225.
[20]G. Bruno, P. Capezzuto, G. Cicala, and P. Manodoro, J. Vac. Sci. Technol. A **12**, 690 (1994).
[21]M. L. Yu, B. N. Eldridge, and R. V. Joshi, *Tungsten Workshop III* (Materials Research Society, Pittsburgh, 1988), p. 75.
[22]M. Hirose, T. Yasakura, and S. Miazaki, Solid State Technol. **12**, 43 (1991).
[23]T. Takahagi, I. Nagai, A. Ishitani, and H. Kuroda., J. Appl. Phys. **64**, 3516 (1988).
[24]V. M. Donnelly, D. L. Flamm, W. C. Dontremont-Smith, and D. J. Werder, J. Appl. Phys. **55**, 242 (1984).
[25]C. G. Van De Walle, Mater. Res. Soc. Symp. Proc. **259**, 375 (1992).
[26]M. L. Yu and B. N. Eldridge, J. Vac. Sci. Technol. A **7**, 625 (1989).

Redistribution subject to AVS license or copyright; see http://scitation.aip.org/termsconditions. Download to IP: 140.113.38.11 On: Thu, 01 May 2014 10:39:31